Journal of the Optical Society of America A
OPTICS, IMAGE SCIENCE, AND VISION

Dual-wavelength polarimeter application in investigations of the optical activity of a langasite crystal

Mykola Shopa,[1,*] Nazar Ftomyn,[2] and Yaroslav Shopa[3,4]

[1]Department of Atomic, Molecular and Optical Physics, Faculty of Applied Physics and Mathematics, Gdańsk University of Technology, Narutowicza 11/12, 80-233 Gdańsk, Poland
[2]Ivan Franko National University of Lviv, 8 Kyrylo and Mefodiy Str., 79005 Lviv, Ukraine
[3]Cardinal Stefan Wyszyński University in Warsaw, 5 Dewajtis Str., 01-815 Warsaw, Poland
[4]Vlokh Institute of Physical Optics, 23 Dragomanov Str., Lviv 79005, Ukraine
*Corresponding author: mszopa@mif.pg.gda.pl

Received 30 December 2016; revised 10 April 2017; accepted 14 April 2017; posted 25 April 2017 (Doc. ID 283805); published 16 May 2017

A method of high-accuracy polarimetry, which includes optical activity measurements' systematic errors, was realized with a dual-wavelength polarimeter for the two wavelengths of 635 and 650 nm. Simultaneous measurements with neighboring wavelengths significantly improved the data processing by increasing the amount of obtained data to eliminate the systematic errors. For a langasite crystal, $La_3Ga_5SiO_{14}$, we measured the temperature dependence of the gyration tensor component g_{11}. Our acquired value does not exceed 0.47×10^{-5} and is much smaller than the previous results obtained by different experimental methods. The results presented in this paper are consistent with the calculated optical rotatory power from the crystal structure data and the polarizabilities of the atoms.

OCIS codes: (120.5410) Polarimetry; (260.5430) Polarization; (260.1180) Crystal optics; (160.4760) Optical properties.

https://doi.org/10.1364/JOSAA.34.000943

1. INTRODUCTION

High-accuracy universal polarimeters (HAUP) [1], which have undergone several modifications and improvements over time [2–6], can be effectively applied to obtain information about the main optical anisotropic parameters of crystals, such as linear birefringence, circular birefringence (also known as optical rotation or optical activity), and linear and circular dichroism. Recently, Mueller matrix polarimetry was successfully applied to the simultaneous measurement of the main optical anisotropic crystal parameters [7–9]. The first experimental data with this method for quartz and achiral $AgGaS_2$ crystals show good results.

Polarimeters allow measuring the optical activity (OA) for light propagation directions distinct from the optical axes, but the results can significantly differ between themselves. The main cause of such discrepancies is systematic errors. Quantitively, one can take them into account by considering the parasitic ellipticities of the polarizer and analyzer: p and q, respectively. These ellipticities (normally of the 10^{-4} order) are usually comparable with eigenwave ellipticities k in crystals, or, sometimes, they can be even bigger than k. The ellipticities are measured as the ratio of the minor to the major axes of the ellipse, which defines a polarization state with two waves [10,11]. Therefore, measurement errors are significant. Experiments [1–5] have shown that systematic errors should be estimated for each experimental process because they depend also on the specimen quality, system alignment, and the precise profile of the laser beam passing through the specimen. Measurements with different crystals keeping all the initial parameters constant lead to varying systematic errors.

An extended laser polarimeter, with a similar design to HAUP but with the implementation of two wavelengths and different principles for data gathering and processing, was designed and applied to investigate the OA of a langasite crystal, $La_3Ga_5SiO_{14}$ (point group 32). The optical properties of these crystals are well studied [12], but the precise value of the OA was acquired along the optical axis only, which corresponds to the gyration tensor component g_{33}. The full detection of OA in uniaxial crystals of this point group requires measurements in the direction perpendicular to the optical axis and calculation of the g_{11} gyration component. There are other uniaxial point groups ($\bar{4}$ and $\bar{4}2m$) of nonenantiomorphous (achiral) uniaxial crystals, which have null OA along the optical axis [10]. For example, the well-known KDP group and $AgGaS_2$ are such types of crystals.

OA is a vital parameter of crystal optical anisotropy and is heavily related to the structural peculiarities of the crystal.

Therefore, we believe that it is important to find the experimental value of OA by means of a dual-wavelength polarimeter and compare it with the results based on the classical polarization model [13].

2. PRINCIPLES OF EXPERIMENT

The polarimetric scheme used for studying the OA in birefringent sections is a polarizer-sample-analyzer (PSA), in which the polarizer azimuth θ and analyzer azimuth χ are measured from the principal crystal axes and are small ($\theta, \chi \ll 1$). Both the polarizer and the analyzer are Glan-type calcite prisms. The measuring procedure is fully automated, with independent rotations of both the polarizer and analyzer, controlled by the stepper motors. In order to measure small intensity changes, the so-called delta-sigma analog-to-digital converter with high resolution is used.

During the experiment, the intensity I transmitted through the PSA system's light is measured as a function of angles $I(\theta, \chi)$. Intensity readings are typically collected for 15–20 values of polarizer azimuths, θ, and for the same amount of analyzer azimuths, χ, close to the position of minimum intensity. These data $I(\chi)$ are then fitted to a biquadratic function using the method of linear least squares, which allows one to find the analyzer azimuth $\chi_{\min}$ that corresponds to the minimum transmission of the polarization system, i.e., $(\partial I/\partial\chi)_\theta = 0$. For a PSA system, the corresponding relation for $\chi_{\min}^{\mathrm{PSA}}(\theta)$ may be expressed as [6,14]

$$\chi_{\min}^{\mathrm{PSA}} = \theta \cos\Gamma + (k - p)\sin\Gamma - \delta\chi, \tag{1}$$

where $\Gamma = 2\pi\Delta n d/\lambda$ is the phase difference, d is the thickness of the specimen, Δn is the linear birefringence, and λ is a wavelength of monochromatic light. One should also define the angular systematic error $\delta\chi$. It is considered that the most likely $\delta\chi$ error is associated with the mechanical elements of the polarimeter [4,5].

In a (θ, χ) coordinate system, the intensity minima azimuths $\chi_{\min}^{\mathrm{PA}}(\theta)$ in the absence of a sample (PA system) form a straight line $\chi_{\min}^{\mathrm{PA}} = \theta$ with a slope angle of 45° (Fig. 1).

In the PSA system, the intensity minima also form a straight line $\chi_{\min}^{\mathrm{PSA}}(\theta)$; however, according to Eq. (1), the tangent of its slope angle is equal to cos Γ. Thus, the optimum scanning area of the analyzer (when $\chi_{\min}^{\mathrm{PSA}}$ is in the middle) depends on the phase difference Γ. Figure 1 shows the surface $I(\theta, \chi)$ cross sections with planes of constant intensities, $I(\theta, \chi) = \mathrm{const}$, which form the so-called HAUP maps in the shape of ellipses [2,15]. The major axes of these ellipses are always tilted by 45° (see maps 1–5 in Fig. 1), but $\chi_{\min}^{\mathrm{PSA}}(\theta)$ tilt angle changes (dashed lines in maps 1–5).

In Fig. 1, the positions of three characteristic polarizer azimuths θ_0 (the invariant azimuth, for which $\chi_{\min}^{\mathrm{PSA}}(\theta_0) = \chi_{\min}^{\mathrm{PA}}(\theta_0)$), θ_1 (corresponds to the global minimum), and θ_2 (corresponds to the minimum light intensity with the crossed polarizers) of the incident light in the PSA system are shown, and the principles of their definition are schematically represented. The relations for these azimuths can be expressed as [6,14]

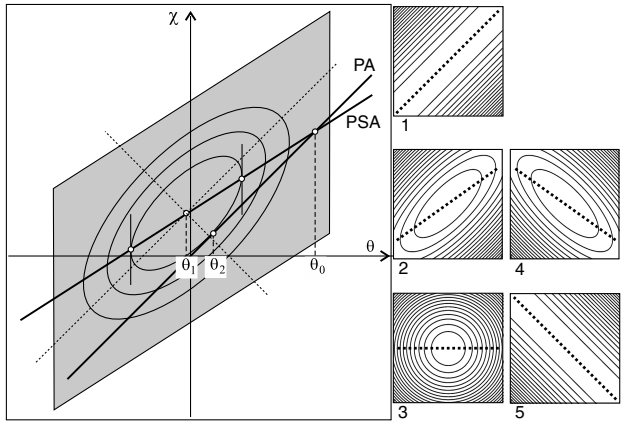

Fig. 1. Characteristic azimuths θ_0, θ_1, and θ_2 for optically active birefringent crystal in (θ, χ) coordinate system. Scanning area of polarizer and analyzer in PSA system is shown as a gray parallelogram. Also, the HAUP map schematic images for different phase differences are presented: 1 - $\Gamma = 2\pi m$, 2 - $\Gamma = \pi/4 + 2\pi m$, 3 - $\Gamma = \pi/2 + 2\pi m$, 4 - $\Gamma = 3\pi/4 + 2\pi m$, and 5 - $\Gamma = (2m + 1)\pi$; m is a natural number.

$$\theta_0 = (k - p)\cot(\Gamma/2) - \delta\chi/(1 - \cos\Gamma), \tag{2}$$

$$\theta_1 = (k - p)\cot\Gamma - (k + q)/\sin\Gamma, \tag{3}$$

$$\theta_2 = -(1/2)(p + q)\cot(\Gamma/2) - \delta\chi/2. \tag{4}$$

Equation (4) is also used in the HAUP method [1–5].

Due to the unknown initial angles between the crystallophysical axes and the azimuth of the polarizer, exact measurements of angles θ_0, θ_1, and θ_2 are not possible. Therefore, we analyze experimentally only their differences: $\Delta\theta_{01} = \theta_0 - \theta_1$, $\Delta\theta_{02} = \theta_0 - \theta_2$, and $\Delta\theta_{12} = \theta_1 - \theta_2$. The relations between θ_0 and θ_1 can be derived from Eqs. (2)–(4):

$$\Delta\theta_{01}\sin\Gamma = 2k - p + q - \delta\chi\cot(\Gamma/2). \tag{5}$$

It is easy to notice that

$$\Delta\theta_{01}(1 + \cos\Gamma) = 2\Delta\theta_{02}; \qquad \Delta\theta_{01}(1 - \cos\Gamma) = -2\Delta\theta_{12}, \tag{6}$$

so determining cos Γ and two of the characteristic azimuths θ_0, θ_1, and θ_2, or one of the differences $\Delta\theta_{01}$, $\Delta\theta_{02}$, and $\Delta\theta_{12}$, is sufficient to get complete data. However, permanent verification of Eq. (6) during the experiment gives us an additional evaluation criterion for the correct measurement procedures. We should remember that the precision of acquired θ_0, θ_1, and θ_2 greatly depends on the phase difference Γ.

By using two sources of light with almost coinciding wavelengths λ_1 and λ_2, we can neglect, in a good approximation, the effects of k value dispersion and assume values p, q, and $\delta\chi$ to be constant. In this dual-wavelength polarimeter, systematic errors can be differently eliminated. In particular, we can have a set of data for characteristic azimuths that were measured in identical conditions but with alternating laser wavelengths. From this point of view, the differences $\Delta\theta_{01}$, $\Delta\theta_{02}$, and $\Delta\theta_{12}$ for separate λ_1 and λ_2 but also the differences $\Delta\theta_{i\lambda} = \theta_i(\lambda_1) - \theta_i(\lambda_2)$, $(i = 0, 1, 2)$ can be successfully analyzed. To increase the

number of measured quantities, we use two orientations of the crystal in the polarization system. It can be achieved by the rotation of the sample 90° around the incident light; then, the signs of Γ and k parameters are reversed [1–3]. The perpendicularity of the sample surface to the incident beam was ensured by adjusting the crystal position so that the beam reflects back to the laser.

Using Eqs. (2)–(4) for the characteristic azimuths, the differences $\Delta\theta_{0\lambda}$, $\Delta\theta_{1\lambda}$, and $\Delta\theta_{2\lambda}$ can be expressed as

$$\Delta\theta_{0\lambda} = A_1(k - p) - B_1\delta\chi, \tag{7}$$

$$\Delta\theta_{1\lambda} = A_2(k - p) - B_2(k + q), \tag{8}$$

$$\Delta\theta_{2\lambda} = -A_1(p + q)/2. \tag{9}$$

Here, we introduced the following notations: $A_1 = \cot(\Gamma_1/2) - \cot(\Gamma_2/2)$, $B_1 = (1 - \cos\Gamma_1)^{-1} - (1 - \cos\Gamma_2)^{-1}$, $A_2 = \cot\Gamma_1 - \cot\Gamma_2$, $B_2 = 1/\sin\Gamma_1 - 1/\sin\Gamma_2$, $\Gamma_1 = \Gamma(\lambda_1)$, and $\Gamma_2 = \Gamma(\lambda_2)$. As a result, the number of equations that can be used to calculate the eigenwave ellipticity k and eliminate the systematic errors is higher when compared to the previously used high-accuracy polarimetric methods.

3. RESULTS AND DISCUSSION

A. Characteristic Azimuth Differences and Systematic Errors

The experiment was performed on (010)-plates of $La_3Ga_5SiO_{15}$ crystal of 2.51 mm thickness in a temperature range from 290 to 370 K. In a dual-wavelength laser polarimeter, we used two semiconductor lasers with neighboring wavelengths of $\lambda_1 = 635$ and $\lambda_2 = 650$ nm. We consider that in Eqs. (1)–(9), none of the quantities except Γ (Fig. 2) depend on the small wavelength change $\delta\lambda = \lambda_2 - \lambda_1 = 15$ nm.

Because the ellipticity k of the eigenwaves does not depend on the specimen thickness, we chose it to be about 2.5 mm. With such thickness, we achieved the optimal change of the phase difference $\Delta\Gamma = 0.65$ in a convenient temperature range of 290–370 K. The temperature of the sample was stabilized with a precision of ±0.5 K, which is enough, considering the slow change of the birefringence Δn with the temperature for langasite crystals.

The experimental temperature dependencies of the characteristic azimuth differences $\Delta\theta_{0\lambda}$, $\Delta\theta_{1\lambda}$, and $\Delta\theta_{2\lambda}$ for the langasite crystal are shown in Fig. 3. As one can see, the differences of the characteristic azimuths become too big compared to the typical value of $k \approx 10^{-4}$. With the considerable change of characteristic azimuths, it is difficult to find the systematic errors p, q, and $\delta\chi$.

We also did not observe contributions from multiple light reflections inside the crystal during our experiments, as, for example, did the authors of [16] during their experiments. If this effect were to take place, then Eq. (6) would not execute correctly, and the slope angles of the major axes of the ellipses on the HAUP maps (Fig. 1) would not be equal to 45°. This fact underlines once again the importance of experimental evaluations of the relations between azimuth differences $\Delta\theta_{01}$, $\Delta\theta_{02}$, and $\Delta\theta_{12}$.

Consecutive analyses of the characteristic azimuths for two wavelengths in stable experimental conditions allow us to find the desired quantities. Figure 4 shows that angles' difference $\Delta\theta_{2\lambda}$ does not depend on the crystal orientation. The sign change of the phase differences Γ_1, Γ_2, and $\Delta\theta_{2\lambda}$ has also been taken into account because the sum of the parasitic ellipticities of the polarizer and analyzer $p + q$ should remain unchanged.

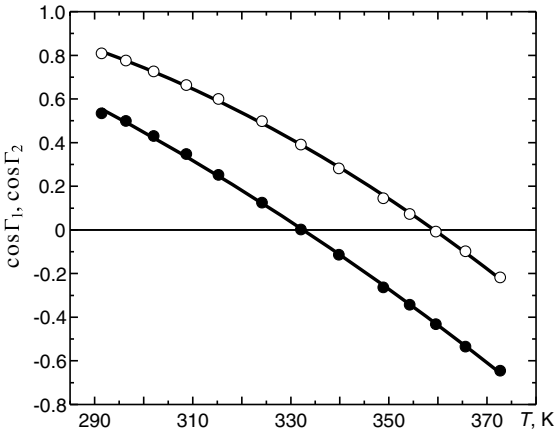

Fig. 2. Temperature dependencies of cos Γ_1 for $\lambda_1 = 635$ nm (○) and cos Γ_2 for $\lambda_2 = 650$ nm (•) acquired from the tangent angle of linear dependences of $\chi_{\min}^{PSA}(\theta)$ on (010)-plates of $La_3Ga_5SiO_{15}$.

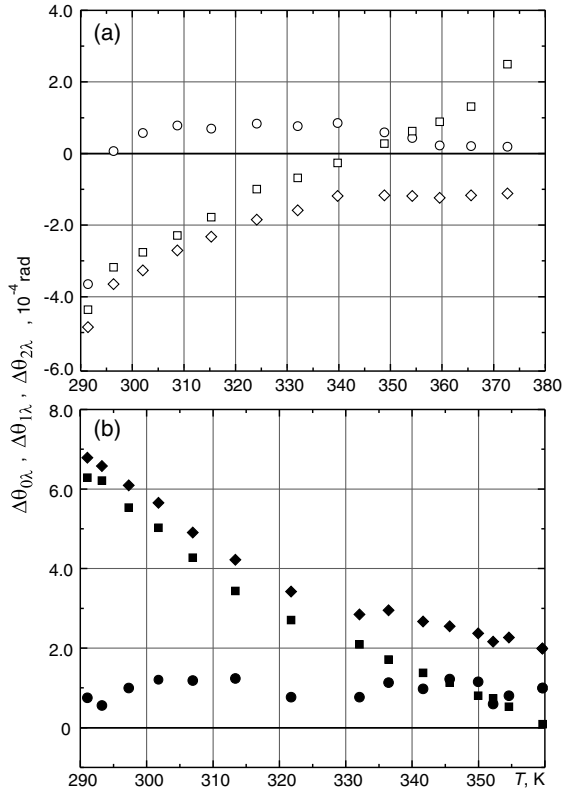

Fig. 3. Dependencies of characteristic azimuths differences $\Delta\theta_{0\lambda}$ (○, •), $\Delta\theta_{1\lambda}$ (□, ■), and $\Delta\theta_{2\lambda}$ (◇, ♦) for LGS crystal on the temperature change for alternative crystal orientations as obtained before (a) and after (b) the 90° rotation of the specimen around the light beam direction.

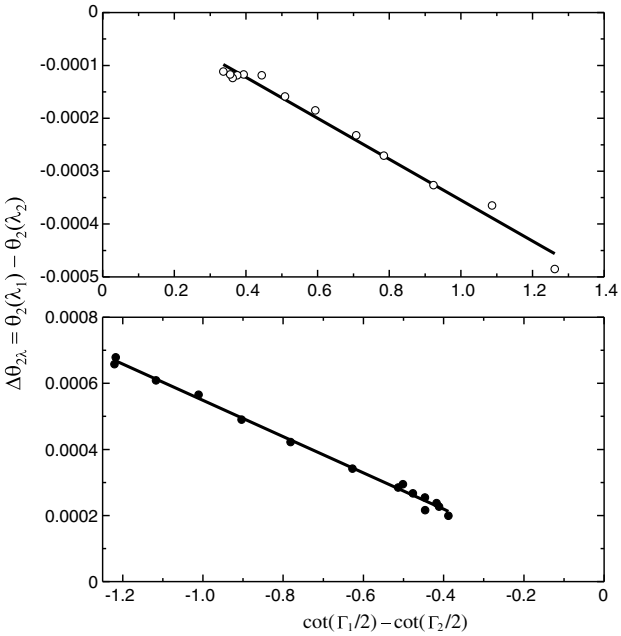

Fig. 4. Dependencies of characteristic azimuths $\Delta\theta_{2\lambda}$ on $\cot(\Gamma_1/2) - \cot(\Gamma_2/2)$ in LGS crystal for alternative crystal orientations as obtained before (∘) and after (•) 90° rotation of the specimen around the light beam direction. The solid lines represent the best linear fit.

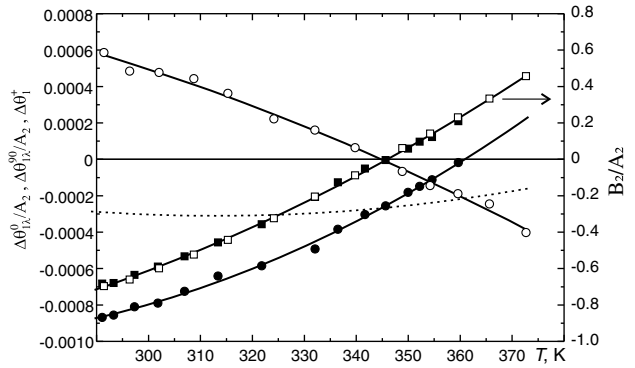

Fig. 5. Two plots of the parameters $\Delta\theta^0_{1\lambda}/A_2$, $\Delta\theta^{90}_{1\lambda}/A_2$ and their sum $\Delta\theta^+_1/A_2$ (short dashed line) versus the temperature T of the LGS crystal corresponding to the alternative crystal orientations before (∘) and after (•) the 90° rotation of the specimen. The points (□, ■) for two crystal setups represent the temperature dependence of the B_2/A_2 values, which change signs at 346 K. The solid lines represent the best second-degree polynomial fits.

For alternative crystal orientations before (0°) and after the 90° rotation of the specimen around the light beam direction, we could find [using Eq. (9)] that for the 0° crystal setup, $p + q = (7.74 \pm 0.28) \times 10^{-4}$ (in radians), and for the 90° crystal setup, $p + q = (11.0 \pm 0.2) \times 10^{-4}$. The difference between these two values is insignificant, and the x- and y-intercepts of the fitted lines are very close to their origin, as follows from Eq. (9).

For further calculations, we used the characteristic azimuth differences $\Delta\theta_{1\lambda}$. By adjusting the temperature of the crystal, we acquired two experimental dependencies [Eq. (8)] for alternative crystal orientations (0° and 90°). Keeping in mind that after the rotation, the eigenwave ellipticity k should change its sign, the sum of the respective characteristic azimuths differences becomes the following:

$$\Delta\theta^+_1 = \Delta\theta^0_{1\lambda} + \Delta\theta^{90}_{1\lambda} = -2pA_2 - 2qB_2. \quad (10)$$

Afterward, by plotting the temperature dependencies $\Delta\theta^0_{1\lambda}/A_2$ and $\Delta\theta^{90}_{1\lambda}/A_2$ (Fig. 5), we calculated the sum of these values $\Delta\theta^+_1/A_2 = -2p - 2qB_2/A_2$ as a result of the addition of second-degree polynomial fitted curves. Figure 5 also represents the temperature dependence of the B_2/A_2 ratio values. This value does not change its sign after the rotation of the crystal, and we get well-matching experimental data for the two crystal setups. This confirms that the 90° rotation procedure of the specimen around the light beam direction was very accurate.

For the data analysis, it is important that at 346 K, the ratio $B_2/A_2 = 0$, and we get just the parasitic ellipticity of the polarizer $p = (1.32 \pm 0.15) \times 10^{-4}$, which, of course, does not depend on the temperature. The values of p and $p + q$ are averaged for the two wavelengths of 635 and 650 nm. So, we get two systematic errors, which are present in Eq. (8). However, the parasitic ellipticity q of the polarizer has two values for different orientations of the crystal $q_0 = (6.42 \pm 0.28) \times 10^{-4}$ and $q_{90} = (9.68 \pm 0.20) \times 10^{-4}$. The difference in values can be explained by the different conditions of the light passing through the PSA system for the two crystal positions. In further calculations, we use the mean value $\overline{q} = (q_0 + q_{90})/2 = (8.05 \pm 0.28) \times 10^{-4}$.

Using Eq. (7), we can find $\Delta\theta^+_0 = \Delta\theta^0_{0\lambda} + \Delta\theta^{90}_{0\lambda} = -2pA_1 - 2\delta\chi B_1$ and the angular error mean value $\delta\chi = -(1.32 \pm 0.40) \times 10^{-4}$. Let us note that in dual-wavelength polarimeters, the determination of the systematic error $\delta\chi$ value is insignificant, while in standard HAUP methods, where this angular error is usually noted as δY, its calculation is important for correct data processing [2–5,14].

B. Optical Activity of LGS Crystal

Langasite family crystals belong to trigonal point group symmetry 32, space group P321; they are uniaxial and optically active. Along the optical axis, the g_{33} component of the gyration tensor is determined by the measurement of the specific rotation ρ.

During the studies of the OA in a plate cut parallel to the optical axis, the gyration tensor component g_{11} is measured. For uniaxial crystals, the relation between g_{11} and the eigenwave ellipticity k is $g_{11} = 2k\Delta n\overline{n}$ [10], where $\overline{n}$ is the mean refractive index. For the mean wavelength of $\lambda = 642.5$ nm, $\overline{n} = 1.905$ [17], and with the channeled spectrum method [18], we acquired birefringence $\Delta n = 0.0116$. We also consider that the influence of the eigenwave ellipticity k dispersion is insignificant. For characteristic azimuth differences, according to Eq. (8), we get

$$\Delta\theta^-_1 = \Delta\theta^0_{1\lambda} - \Delta\theta^{90}_{1\lambda} = 2k(1 - B_2/A_2). \quad (11)$$

This allows us to find $k = (1.3 \pm 0.4) \times 10^{-4}$ for the temperature of 346 K. As one can see, the eigenwave ellipticity is significantly smaller then the parasitic ellipticities p and q; therefore, the calculation error of k is substantial and depends

mostly on the experimental precision of the characteristic azimuths and phase differences Γ for both wavelengths, which influence A_2 and B_2.

Nevertheless, taking into account the systematic errors grants the chance for consecutive calculations of OA perpendicular to the optical axis of the crystal. The temperature dependencies of the g_{11} components of the gyration tensor derived from the two measurements of the eigenwave ellipticity k are shown in Fig. 6. The presented results of calculations take into account Eq. (8), values p and q, and also the temperature-dependent mean refractive index and birefringence.

From the linear fitting of our data for the temperature of 295 K, we get the value $g_{11} = (0.47 \pm 0.17) \times 10^{-5}$, which is much smaller than that given in [17,19]. These values of OA were determined by the spectral measurement of the amplitude of oscillations of the rotation angle χ of the major axis of the ellipse of the passing light polarization. Such a method assumes that the polarizer is perfect (parasitic ellipticity $p = 0$), is stationary during the experiment, and that its input azimuth should be $\theta = 0$. Then, according to Eq. (1), $\chi = k \sin \Gamma$ and $\chi = \pm k$ for wavelengths for which $\sin \Gamma = \pm 1$. In [17], the gyration tensor component $g_{11} \approx 4.0 \times 10^{-5}$, so the corresponding ellipticity $k = 9.1 \times 10^{-4}$ for $\lambda = 633$ nm. If this much larger ellipticity was real, it would have prominently emerged on the dependences shown in Figs. 3 and 5.

Previous data [6] should also be treated critically, because the use of a reference crystal for measuring the parasitic ellipticity p often gives incorrect results. Our current method does not use the reference crystal, because earlier it was established that a measurement with different samples gives different values of parasitic errors [4,5]. Therefore, we used only the rotation of the sample during the experiment, and it allowed us to include the systematic errors more accurately. The earlier results obtained for the LGS crystal did not consider such errors and, in our opinion, this fact had a negative impact on the results acquired in [6].

Using formally the relation $\rho_\perp = \pi g_{11}/(\lambda n_e)$ for the specific rotation [10] perpendicular to the optic axis, we get $\rho_\perp = 0.73$ deg/mm compared to $\rho = -3.3$ deg/mm in the direction of the optical axis [17].

The structure of a langasite crystal does not contain screw axes. Its OA is connected with helical formations of the electron density, imitating the screw axis [20]. Therefore, in the direction of the optical axis, specific rotations in the LGS are almost 6 times smaller than those in α quartz SiO_2.

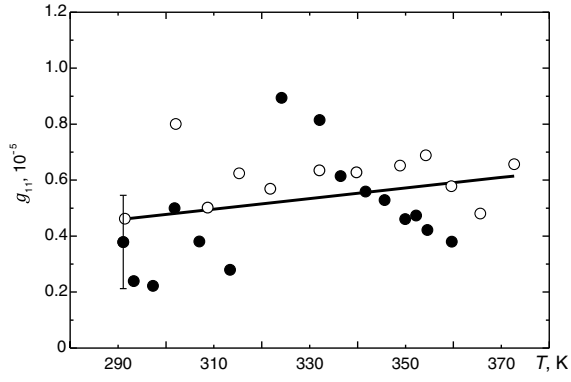

Fig. 6. Temperature dependencies of g_{11} components of the gyration tensor for the LGS crystal before (∘) and after (•) the 90° rotation of the sample. The error bar shows the goodness of linear fit.

We would like to compare our results of polarimetric experimental data with the calculated ones (the calculation method described in [13]). Using the same values of polarizability volumes [21] ($\alpha_{La} = 1,886$ Å^3, $\alpha_{Ga} = 0,375$ Å^3, $\alpha_{Si} = 0,050$ Å^3, and $\alpha_O = 1,740$ Å^3), we obtained $\rho_\perp = 1.1$ deg/mm. Unfortunately, this result is inaccurate, because ρ and $\rho_\perp$ should be opposite in sign (according to the gyrotropic properties of crystals with point group symmetry 32). Langasite crystals have the smallest OA among the langasite family [22]. With such crystal properties, it is hard to expect the theoretical calculations within the classical OA model to be accurate. Small changes of the polarizability volumes influence the results significantly. One can only estimate the OA value, which we have accomplished. Nevertheless, we have attempted to verify theoretically whether our experimental results are correct.

In contrast, these calculating techniques were applied with success to pure $Ca_3Ga_2Ge_4O_{14}$ crystals (langasite family) [23]. As a result, values of electronic polarizability volumes should be specified for studied LGS crystals. It is interesting to note that some crystals with a langasite structure show unusually large values of the specific rotation when compared to LGS [24].

Finally, it should be noted that almost all langasite family crystals are disordered; therefore, precise structure data and correct values of electronic polarizability volumes are necessary for consequent calculations.

4. CONCLUSIONS

We used the extended HAUP polarimetric method by using two neighboring laser wavelengths and applied a new method for the elimination of systematic errors in the measurement of OA in directions perpendicular to the optical axis of a crystal. The acquired value of the eigenwave ellipticity k is significantly smaller than the systematic errors, which are caused by the polarizer's imperfections. Nevertheless, we were able to find systematic errors and calculate the temperature dependence of the g_{11} component of the gyration tensor. The dual-wavelength HAUP polarimetric method avoids the influence of angular errors, which play a major perturbation role in the standard HAUP method. The OA of langasite crystals perpendicular to the optical axis turned out to be significantly lower than the OA along the z-axis.

REFERENCES

1. J. Kobayashi and Y. Uesu, "A new optical method and apparatus HAUP for measuring simultaneously optical activity and birefringence of crystals. I. Principles and construction," J. Appl. Crystallogr. **16**, 204–211 (1983).
2. J. Moxon and A. Renshaw, "Improved techniques for the simultaneous measurement of optical activity and circular dichroism in birefringent crystal sections," Z. Kristallogr. **185**, 636–655 (1988).
3. E. Dijkstra, H. Meekes, and M. Kremers, "The high-accuracy universal polarimeter," J. Phys. D **24**, 1861–1868 (1991).
4. C. L. Folcia, J. Ortega, and J. Etxebarria, "Study of the systematic errors in the HAUP measurements," J. Phys. D **32**, 2266–2277 (1999).
5. C. Hernández-Rodríguez, P. Gomez-Garrido, and S. Veintemillas, "Systematic errors in the high-accuracy universal polarimeter: application to the determining temperature-dependent optical anisotropy

of KDC and KDP crystals," J. Appl. Crystallogr. **33**, 938–946 (2000).
6. Y. Shopa and M. Kravchuk, "Study of optical activity in $La_3Ga_5SiO_{14}$ with high-accuracy polarimetric methods," Phys. Stat. Solidi A. **158**, 275–280 (1996).
7. O. Arteaga, A. Canillas, and G. E. Jellison, "Determination of the components of the gyration tensor of quartz by oblique incidence transmission two-modulator generalized ellipsometry," Appl. Opt. **48**, 5307–5317 (2009).
8. O. Arteaga, J. Freudenthal, and B. Kahr, "Reckoning electromagnetic principles with polarimetric measurements of anisotropic optically active crystals," J. Appl. Crystallogr. **45**, 279–291 (2012).
9. O. Arteaga, "Spectroscopic sensing of reflection optical activity in achiral $AgGaS_2$," Opt. Lett. **40**, 4277–4280 (2015).
10. J. F. Nye, *Physical Properties of Crystals: Their Representation by Tensors and Matrices* (Oxford Universtiy, 1985).
11. A. Yariv and P. Yeh, *Optical Waves in Crystals: Propagation and Control of Laser Radiation* (Wiley, 2002).
12. W. T. Arkin, *New Research on Lasers and Electro-Optics* (Nova Science, 2007).
13. V. Devarajan and A. Glazer, "Theory and computation of optical rotatory power in inorganic crystals," Acta Crystallogr. Sect. A **42**, 560–569 (1986).
14. Y. Shopa, "High accuracy polarimetry and its application," Ukr. J. Phys. Opt. **2**, 58–75 (2001).
15. Y. Shopa and N. Ftomyn, "Polarimetric studies of linear dichroism in Cr-doped gallogermanate crystals," Ukr. J. Phys. Opt. **7**, 183–188 (2006).
16. C. Hernández-Rodríguez and P. Gomez-Garrido, "Optical anisotropy of quartz in the presence of temperature-dependent multiple reflections using a high-accuracy universal polarimeter," J. Phys. D **33**, 2985–2994 (2000).
17. A. A. Kaminskii, B. V. Mill, G. G. Khodzhabagyan, A. F. Konstantinova, A. I. Okorochkov, and I. M. Silvestrova, "Investigation of trigonal $(La_{1-x}Nd_x)_3Ga_5SiO_{14}$ crystals," Phys. Stat. Solidi. A **80**, 387–398 (1983).
18. J. W. Ellis and L. Glatt, "Channeled infra-red spectra produced by birefringent crystals," J. Opt. Soc. Am. **40**, 141–142 (1950).
19. B. N. Grechushnikov and A. F. Konstantinova, "Crystal optics of absorbing and gyrotropic media," Comput. Math. Appl. **16**, 637–655 (1988).
20. A. P. Dudka and B. V. Mill', "Accurate crystal-structure refinement of $Ca_3Ga_2Ge_4O_{14}$ at 295 and 100 K and analysis of the disorder in the atomic positions," Crystallogr. Rep. **58**, 594–603 (2013).
21. Y. Shopa, N. Ftomyn, and I. Sokoliuk, "Crystal structure and optical activity of $La_3Ga_5SiO_{14}$ crystals," Ukr. J. Phys. Opt. **15**, 155–161 (2014).
22. A. F. Konstantinova, T. G. Golovina, B. V. Nabatov, A. P. Dudka, and B. V. Mill, "Experimental and theoretical determination of the optical rotation in langasite family crystals," Crystallogr. Rep. **60**, 907–914 (2015).
23. Y. Shopa and N. Ftomyn, "Optical activity of $Ca_3Ga_2Ge_4O_{14}$ crystals: experiment and calculus," Opt. Appl. **43**, 217–228 (2013).
24. Q. Haifeng, W. Aijian, and Y. Duorong, "Investigation on giant optical activity of piezoelectric crystals with langasite structure," Mater. Sci. Eng. B **117**, 143–145 (2005).